Gigahertz surface acoustic wave generation on ZnO thin films deposited by radio frequency magnetron sputtering on III-V semiconductor substrates

Qi Jie Wang,[a] Christian Pflügl, William F. Andress, Donhee Ham, and Federico Capasso[b]
School of Engineering and Applied Sciences, Harvard University, Cambridge, Massachusetts 02138

Masamichi Yamanishi
Central Research Laboratories, Hamamatsu Photonics K.K., Shizuoka 434-8601, Japan

(Received 10 July 2008; accepted 8 September 2008; published 3 November 2008)

The authors demonstrate 1.6 GHz surface acoustic wave (SAW) generation using interdigital transducers patterned by e-beam lithography on a thin ZnO piezoelectric film deposited on an InP substrate. The highly oriented, dense, and fine-grain ZnO film with high resistivity was deposited by radio frequency magnetron sputtering and was characterized by x-ray diffraction, scanning electron microscopy, atomic force microscopy, and a four-point probe station. The acoustic wavelength of the 1.6 GHz SAW generated by exciting the interdigital transducer on ZnO/InP with a microwave signal is 1.6 μm. This SAW filter device could be monolithically integrated with optoelectronic devices, opening new opportunities to use SAWs for applications such as gigahertz-frequency filters on optoelectronic devices and novel widely tunable quantum cascade lasers. © *2008 American Vacuum Society.* [DOI: 10.1116/1.2993176]

I. INTRODUCTION

Surface acoustic wave (SAW) devices have been widely used in wireless communications and signal processing application.[1] Currently, there is a growing interest to use SAWs in optoelectronics for optical and/or electrical modulations. By directly generating SAWs on III-V semiconductors, and using them for modulating the electrical and/or the optical properties such as the free carrier distribution and the optical mode, one can achieve useful device functionalities in low-dimensional electron systems,[2–6] photonic crystal structures,[7] and optical cavities.[8]

Efficient generation of SAWs at frequencies above 1 GHz on III-V semiconductors would not only broaden the area of compact system-on-a-chip solutions for wireless communication, high-frequency filtering, and sensing applications, but would also provide interesting opportunities for monolithically integrated SAW-modulated optoelectronic devices because the acoustic wavelengths corresponding to frequencies beyond 1 GHz are comparable to the wavelengths of midinfrared light in semiconductor. This allows direct modulation of semiconductor devices such as quantum cascade lasers (QCLs) to produce a single-mode broadly tunable laser output.[9] The mechanism is the periodic modulation of the carrier density and thus of the optical gain leading to distributed feedback laser action by the acoustic wave propagating along the QCL cavity. The wavelength of the laser output could then be easily tuned by changing the frequency of the acoustic wave. This, however, has so far been difficult due to the weak piezoelectricity and low acoustic phase velocities of III-V semiconductor materials.

A solution for gigahertz SAW generation on III-V semiconductors may be found by depositing a thin film of a highly piezoelectric material such as ZnO on the III-V semiconductor devices.[10,11] In this scenario, high crystalline quality and smooth surface morphology of the thin film are crucial to attain efficient SAW excitation and to reduce SAW propagation losses. This is especially important at high frequencies because losses increase with SAW frequency.

To generate SAWs, interdigital transducers (IDTs) consisting of an array of metal fingers deposited on the surface of samples are usually employed.[1] By fabricating IDTs on the surface of thin ZnO films on substrates with high phase velocities, such as glass or sapphire,[12] SAW devices with frequencies above 1 GHz have been demonstrated. In contrast, the acoustic phase velocity of III-V semiconductors is low with a typical value of 2500–3000 m/s. In order to achieve a SAW frequency of 2 GHz, a periodic length of 1.25–1.5 μm of IDTs corresponding to a finger width of single IDT structure of 300–400 nm must be achieved, but this reaches the limitation of conventional photolithography resolution. With the conventional photolithography approach, up to 360 MHz SAW devices on ZnO/GaAs layered structure have been demonstrated in Ref. 13. However, there are no reports on the generation of SAWs above 1 GHz by fabricating IDTs on a highly piezoelectric film deposited on III-V semiconductors, such as GaAs and InP. Although few reports using different approaches, such as using embedded IDTs (Ref. 14) in GaAs and an acoustic mode converter of bulk acoustic waves into SAWs (Ref. 15) defined by holography, are available.

In this article, we report the generation of 1.6 GHz SAWs by using IDTs on a high quality ZnO thin film, which is deposited on an InP (100) substrate using radio frequency magnetron sputtering technique. The growth parameters of

[a]Electronic mail: qijie@seas.harvard.edu
[b]Electronic mail: capasso@seas.harvard.edu

Author complimentary copy. Redistribution subject to AIP license or copyright, see http://jvb.aip.org/jvb/copyright.jsp

TABLE I. Optimal sputtering conditions for ZnO thin films.

Target	ZnO
O_2:Ar gases	20:60
Pressure	7×10^{-3} Torr
Substrate temperature	200 °C
Deposition rate	~100 nm/h
Power	100 W

ZnO film are optimized to produce a highly oriented, dense, and fine-grain ZnO film with high resistivity. The gigahertz IDTs are patterned on the ZnO film using an e-beam lithography process, which is optimized to overcome charge accumulation on the semi-insulating ZnO surface.

II. EXPERIMENT

A. ZnO thin film deposition

The ZnO thin film was deposited with a rf magnetron sputtering system (AJA ATC 2000 UHV) on a (100) oriented Fe-doped semi-insulating InP substrate with a thickness of 500 μm and a resistivity of more than 10^7 Ω cm. The size of the ZnO sputter target is 2 in. in diameter and 0.125 in. thick, and the purity of which is 99.995%. The sputtering process conditions were optimized to yield a polycrystalline ZnO film with the *c*-axis perpendicular to the surface in order to achieve a high piezoelectricity, a high resistivity, and a smooth film surface. In this way, we were able to generate strong SAW fields on the weak piezoelectric III-V (InP) semiconductor by using IDTs. The optimized conditions that include optimal composition of gases, gas pressure, and substrate temperature are shown in Table I. The growth rate is around 100 nm/h, and the thickness of the fully grown ZnO thin film is 250 nm. After the sputtering, the ZnO thin film was annealed in vacuum at a temperature of 400 °C for an hour in order to improve the ZnO film quality.[16] In the experiment, we observed the (002) peak intensity of the x-ray diffraction (XRD) data increased by about 10% after annealing, while the full width at half maximum (FWHM) of the (002) peak was almost the same. Figure 1 shows a measured XRD pattern of the sputtered ZnO thin film under the optimized sputtering condition. The 2θ peak appears at 34.47°, which corresponds to ZnO (002) preferred orientation. In addition to the main (002) peak, we also observed other weak ZnO peaks related to (101) orientation at 36.05° and (110) orientation at 56.62° with XRD intensities at least ten times lower than the main (002) peak. The FWHM of the peak is 0.22°. The resistivity of the sputtered ZnO thin film measured with a four-point probe system is on the order of 10^{10} Ω cm which is sufficient to prevent current leakage between transducer fingers.

Figure 2(a) is a scanning electron microscope (SEM) side-view image of a cleaved ZnO/InP sample showing the dense microstructure of the sputtered ZnO film. The surface morphology of the ZnO film is observed with an atomic force microscopy (AFM) system (Asylum MFP-3D). A granular film surface with a film thickness around 250 nm is clearly observed in the AFM image in Fig. 2(b). Although there are pyramid grains appearing on the surface, the lateral grain sizes are well below 100 nm. The height of these pyramid grains is below 20 nm resulting in an average surface rough-

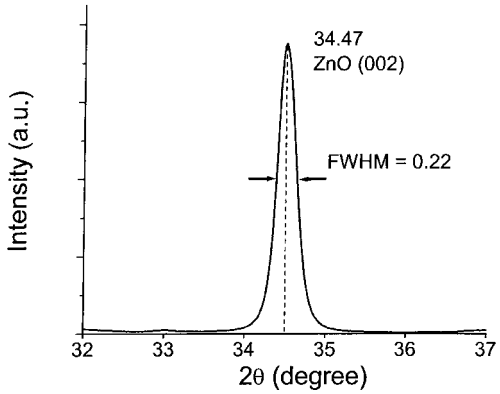

FIG. 1. X-ray diffraction pattern of a sample with ~250 nm thick ZnO thin film on InP substrate grown by radio frequency magnetron sputtering. The FWHM of the main peak at 34.47° degree corresponding to (002) orientation is 0.22°.

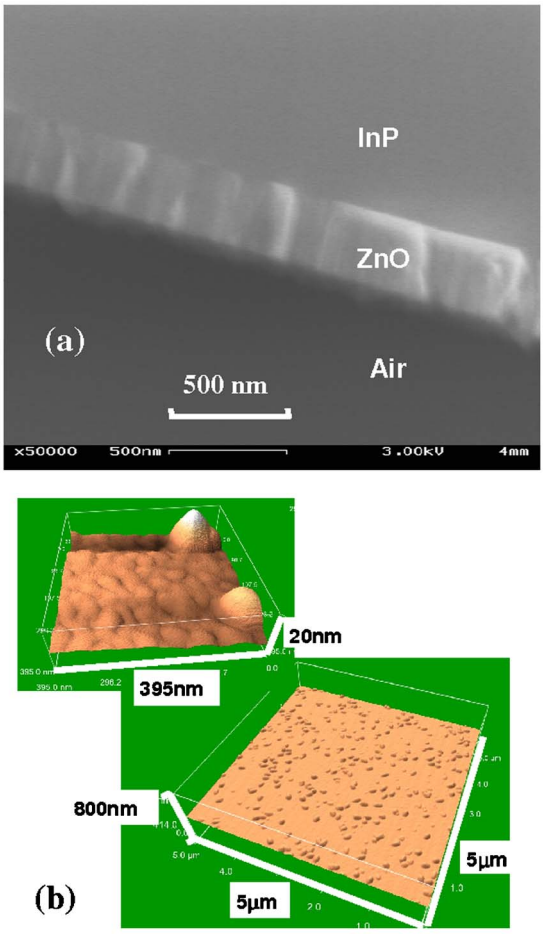

FIG. 2. (a) Scanning electron microscope side view of a cleaved ZnO/InP sample; (b) atomic force microscopy image of the deposited ZnO film surface on InP substrate; the inset shows the enlarged image of the ZnO film surface.

Author complimentary copy. Redistribution subject to AIP license or copyright, see http://jvb.aip.org/jvb/copyright.jsp

ness below 6 nm across the entire film, as shown in the inset of Fig. 2(b). The smoothness of the surface is sufficient to sustain low-loss SAW propagation at high frequencies, and also to deposit metal electrodes for IDTs with a finger width of several hundred nanometers onto the surface of the ZnO film surface.

B. SAW device fabrication

We fabricated IDTs in a single-finger structure to achieve SAWs with a central frequency of around 1.6 GHz corresponding to the IDT's periodic length of about 1.6 μm. The finger width was 400 nm designed to be the same as the spacing between the IDT fingers. The IDTs were fabricated using e-beam lithography followed by a standard lift-off technique. Due to the high resistivity of the ZnO/InP layered structure, charges accumulate on the top surface of the sample during the e-beam lithography process. To avoid this, we adopted a fabrication procedure slightly different from the one reported in Ref. 17. First, we spun a double layer resist coating for the lift-off process, then deposited a 10 nm layer of Cr on the top, whereas an Al film is used directly above AlN for charge evacuation purposes, as discussed in Ref. 17. Depositing the Cr film on top of the resist is necessary to avoid etching the ZnO thin film when etching the Cr film, because ZnO films are etched rapidly in almost all acids.[18] The double layer resist coating consists of two different electron sensitive resists, 495PMMA A4 (Micro Chem) and 950PMMA A4 (Micro Chem). The e-beam lithography was done at an acceleration voltage of 30 kV, electron current of 65 pA, magnification of 450, and exposure dose of 300 μC/cm^2. After the lithography, the Cr thin film was etched with Cyantek CR-7 etching solution, then the resist was developed in a methyl-isobutyl-ketone:isopropanol (1:3) solution for 70 s and rinsed with isopropanol. Next, a metal electrode for IDTs of Ti/Au (10/60 nm) was deposited by e-beam evaporation, followed by a lift-off process in acetone. Figure 3(a) shows the SEM picture of the fabricated transducer with a finger width of 400 nm on top of ZnO/InP substrate. With e-beam lithography, the error of finger width is within 5%. The number of IDT finger pairs is 50 and the dimension of the input/output transducer is about 70 μm wide and 80 μm long.

III. RESULTS AND DISCUSSIONS

Figure 3(b) shows the layout of the experimental setup used to measure the frequency response of the SAW device. One transducer was used as an input to launch acoustic waves along the $(0\,\bar{1}\,1)$ direction of the InP surface. The second transducer served as a receiver at a propagation distance of ~500 μm. The propagation distance is defined as the distance between the center of the input and the center of the output transducers. The input transducer was driven by a rf signal source (Agilent 83650L) spanning a frequency range from 1.55 to 1.65 GHz with an input power of 100 mW from the signal source. The measured SAW filter response with a spectrum analyzer (E4448A) is shown in Fig. 4. It shows that the SAW device has a central frequency f_a of

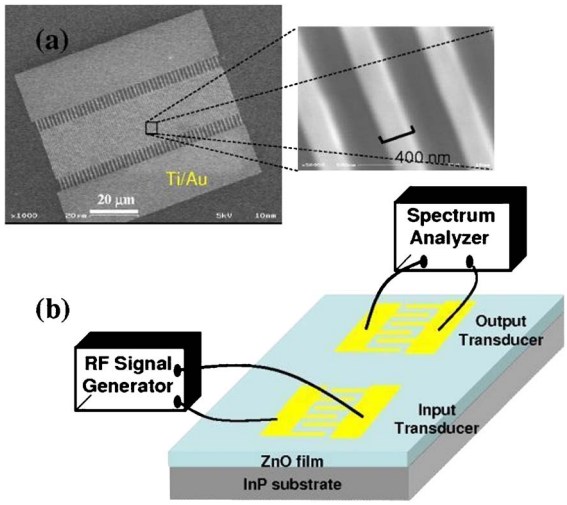

FIG. 3. (a) Scanning electron microscope picture of an e-beam defined transducer with a finger width of 400 nm and a period of 50; (b) layout of the measurement setup, showing the geometry of the input and output transducers on the ZnO/InP sample.

about 1.58 GHz and the bandwidth of the filter response is about 50 MHz. The SAW phase velocity over the ZnO/InP layer structure is estimated to be $f_a \times \lambda_a = 2528$ m/s, where λ_a is the wavelength of the acoustic wave. The input and output transducers were connected to the rf signal source and the spectrum analyzer, respectively, using a microwave probe station (M150, Cascade Microtech. Inc.). The measured loss of the entire setup, defined as the ratio of the output power at the central frequency measured by spectrum analyzer to the input power read from the signal source, is around 46 dB which includes losses from IDTs and propagation loss. It is noted that the IDTs in the current study are not optimized. Improvement of the filter performance in term of the passband bandwidth and passband extinction ratio could be attained by optimizing the IDT structure, for example, by using split-finger structure.[1]

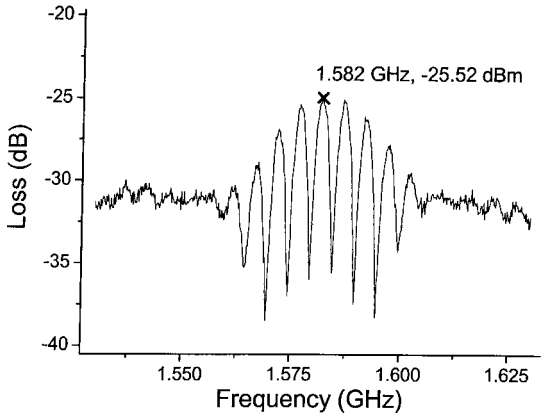

FIG. 4. Measured SAW spectrum response centered at ~1.6 GHz with a broadband spectrum analyzer; the interference pattern is due to the Fabry-Pérot-type resonance formed between the input and output transducers with a periodicity of ~5 MHz.

Author complimentary copy. Redistribution subject to AIP license or copyright, see http://jvb.aip.org/jvb/copyright.jsp

It can be seen from Fig. 4 that there is an interference pattern in the spectrum, with a periodicity of about 5 MHz. We attribute this interference phenomenon to the beating between the acoustic and electromagnetic waves received by the output transducer. The relatively high noise level outside of the SAW transmission bandwidth is caused by the received electromagnetic wave. The high extinction ratio of the interference pattern within the SAW transmission bandwidth is due to the beating between the received electromagnetic and acoustic waves. In this mechanism, the period of the interference is the ratio of the acoustic velocity over the SAW transmission distance. Considering the measured acoustic velocity is around 2528 m/s and the separation distance is 500 μm, we calculated the expected period the interference pattern to be around 5 MHz which matches the experimental results very well.

SAW propagation loss is a very important parameter to characterize the SAW devices. For the fabricated SAW devices at 1.6 GHz in this study, the SAW propagation loss was estimated by fabricating SAW devices with the same central frequency of 1.6 GHz but using different separation distances (600 μm and 1.1 mm) between the input and output transducers. The total losses of the SAW devices with a transducer separation distance of 600 μm and 1.1 mm were about −52 and −57 dB, respectively. From these measurements we estimated the SAW propagation loss at 1.6 GHz to be around 10 dB/mm. Besides the SAW propagation loss, electromechanical coupling coefficient K^2 is another important factor for SAW devices, which strongly depends on the film thickness, and can be calculated from the measured impedance of the IDTs.[19] For the IDTs that were used to generate 1.6 GHz SAW, we measured impedance characteristics of the IDTs with respect to frequency by using a network analyzer (E8364A). The coupling coefficient K^2 deduced from these measurements is ~0.2%. By optimizing the geometry of IDTs and the thickness of the ZnO thin film,[12] one can further increase the coupling coefficient K^2 and match the impedance of the device to that of the signal source.

IV. CONCLUSION

In conclusion, we have presented the fabrication and measurement of 1.6 GHz SAW devices on an InP substrate, by using ZnO thin films to enhance the piezoelectricity, and using e-beam lithography for the fabrication of IDTs. The high quality ZnO thin film is grown by radio frequency magnetron sputtering system with optimized growth parameters. The approach is applicable to the generation of gigahertz SAW on III-V semiconductor systems which has much potential in applications such as acoustic charge transport, acoustic modulation of photonic crystal structures, and monolithic integration of SAW devices with optoelectronic devices.

ACKNOWLEDGMENTS

The authors acknowledge financial support from Hamamatsu Photonics K.K., Japan. This work was performed in part at the Center for Nanoscale Systems (CNS), a member of the National Nanotechnology Infrastructure Network (NNIN), which is supported by the National Science Foundation under NSF Award No. ECS-0335765. CNS is part of the Faculty of Arts and Sciences at Harvard University.

[1] C. K. Campbell, *Surface Acoustic Wave Devices for Mobile and Wireless Communications* (Academic, New York, 1998).
[2] A. Wixforth, J. Scriba, M. Wassermeier, J. P. Kotthaus, G. Weimann, and W. Schlapp, Phys. Rev. B **40**, 7874 (1989).
[3] A. O. Govorov, A. V. Kalameitsev, M. Rotter, A. Wixforth, J. P. Kotthaus, K.-H. Hoffmann, and N. Botkin, Phys. Rev. B **62**, 2659 (2002).
[4] M. Rotter, A. V. Kalameitsev, A. O. Govorov, W. Ruile, and A. Wixforth, Phys. Rev. Lett. **82**, 2171 (1999).
[5] T. Sogawa, P. V. Santos, S. K. Zhang, S. Eshlaghi, A. D. Wieck, and K. H. Ploog, Phys. Rev. Lett. **87**, 276601 (2001).
[6] J. R. Gell*et al.*, Appl. Phys. Lett. **89**, 243505 (2006).
[7] M. M. de Lima, Jr. and P. V. Santos, Rep. Prog. Phys. **68**, 1639 (2005).
[8] M. M. de Lima, Jr., R. Hey, and P. V. Santos, Appl. Phys. Lett. **83**, 2997 (2003).
[9] M. V. Kisin and S. Luryi, Appl. Phys. Lett. **82**, 847 (2003).
[10] S. J. Chang, Y. K. Su, and Y. P. Shei, J. Vac. Sci. Technol. A **13**, 381 (1995).
[11] E. Vasco, J. R. Zuazo, L. Vazquez, C. Prieto, and C. Zaldo, J. Vac. Sci. Technol. B **19**, 224 (2001).
[12] M. Kadota, T. Miura, and M. Minakata, J. Cryst. Growth **237**, 523 (2002).
[13] Y. Kim, W. D. Hunt, F. S. Hickernell, and R. J. Higgins, J. Appl. Phys. **75**, 7299 (1994).
[14] M. M. de Lima, Jr., W. Seidel, H. Kostial, and P. V. Santos, J. Appl. Phys. **96**, 3494 (2004).
[15] M. Yamanishi, M. Ameda, K. Ishii, T. Kawamura, K. Tsubouchi, and N. Mikoshiba, Appl. Phys. Lett. **33**, 251 (1978).
[16] R. J. Lad, P. D. Funkenbusch, and C. R. Aita, J. Vac. Sci. Technol. **17**, 808 (1980).
[17] P. Kirsch, M. B. Assouar, O. Elmazria, V. Mortet, and P. Alnot, Appl. Phys. Lett. **88**, 223504 (2006).
[18] J. Sun, J. Bian, H. Liang, J. Zhao, L. Hu, Z. Zhao, W. Liu, and G. Du, Appl. Surf. Sci. **253**, 5161 (2007).
[19] G. D. O'Clock, Jr. and M. T. Duffy, Appl. Phys. Lett. **23**, 55 (1973).

Author complimentary copy. Redistribution subject to AIP license or copyright, see http://jvb.aip.org/jvb/copyright.jsp